Structural-Functional Characterization of Degradation Mechanisms in Low Bandgap Polymer-Fullerene OPV Devices

Eric Muckley
Bredesen Center, University of Tennessee Knoxville
Center for Nanophase Materials Sciences, Oak Ridge National Laboratory

August 2015

Abstract

Polymer-fullerene bulk heterojunction (BHJ) organic photovoltaics (OPVs) show enormous promise for low cost renewable energy production. In an effort to increase device efficiencies, recent attention has turned toward the utilization of low bandgap conjugated polymers for photon harvesting. However, the stability of devices based on low bandgap materials remains poorly understood and represents one of the primary roadblocks for widespread OPV commercialization. Developing a systematic approach for studying degradation mechanisms in low bandgap OPVs is critical for improving device lifetimes. In this study, an experimental procedure for identifying the specific location and trigger of different degradation mechanisms is outlined. Emphasis is placed on in situ structural-functional characterization of different device materials under a variety of environmental conditions with a focus on machine learning techniques for flexible data analysis.

Contents

1 Introduction

Interest in organic photovoltaics (OPVs) has grown rapidly in recent years because of their low cost, light weight, and mechanical flexibility.[1–4] The bulk heterojuction (BHJ) device architecture has gained particular attention because of its simple fabrication process and high power conversion efficiency (PCE), which is currently approaching 10%.[5] The photoactive layer of a typical BHJ device consists of a blend of electron-donating conjugated polymers and electron-accepting fullerenes or fullerene derivatives.[6] After film deposition of the solution-based blend, spontaneous phase separation between polymer and fullerene domains results in the formation of nanoscale heterojunctions throughout the film, giving rise to a large donor-acceptor (D-A) interfacial area.[7] Since exciton binding energies in organic semiconductors (0.1-1 eV) are several orders of magnitude higher than those in inorganic semiconductors (∼1 meV), the strong electric field at the D-A interface is required for exciton dissociation in OPVs.[2,6] BHJ structures contain polymer-fullerene domain interfaces which are separated by distances less than the exciton diffusion length (10-15 nm in most organic semiconductors), which enables efficient exciton dissociation and higher PCE than bilayer heterojunction devices.[8]

Commonly employed polymers poly(1,4-phenylene-vinylene) (PPV) and poly-(3-hexylthiophene) (P3HT) have enabled laboratory-scale organic BHJ devices to achieve PCEs $> 6\%$ over the last decade.[7] However, it is widely agreed that two milestones must be met before OPV production can become commercially viable: device PCE must exceed 10%, and outdoor device lifetimes must excede 5 years.[7,9–11] In efforts to achieve and surpass a 10% PCE, attention has turned toward tuning of the optical properties of photoactive materials. The optical bandgap in most organic semiconductors is twice that of silicon (∼1.1 eV), which restricts light harvesting by OPVs to wavelengths above 650 nm, resulting in utilization of less than 23% of the solar spectrum by P3HT-based BHJ devices.[2,12,13] While typical OPV devices now exhibit internal quantum efficiencies (IQEs) of 70% or higher for blue photons, efficient energy conversion of red photons can not be achieved unless polymers with smaller optical bandgaps (∼1.5 eV) are used for photon harvesting.[14] It is critical that OPVs exhibit strong absorption in the visible range (390-700 nm) because this accounts for 54% of the energy in solar radiation under AM1.5 conditions.[7,15] Since fullerenes such as [6,6]-phenyl-C61-butyric acid methyl ester (PCBM) which exhibit weak visible light absorption are commonly used as electron acceptor materials in BHJ devices, the polymer donor is generally responsible for photon collection.[16]

To utilize a larger region of the solar spectrum, efforts have focused on the development and utilization of low bandgap polymers such as poly(2,7-carbazole) derivatives. These materials are particularly attractive because their bandgap energies can be tuned by coupling the polymer to different electron-deficient moieties. One poly(2,7-carbazole) derivative family, poly[N-9'-hepta-decanyl-2,7-carbazole-alt-5,5-(4',7'-di-2-thienyl-2',1',3'-benzothiadiazole) (PCDTBT), exhibits an IQE of nearly 100% in the visible range.[7,17] Another low bandgap polyer which has received recent attention is poly[4,8-bis-substituted-benzo[1,2-b:4,5-b0]dithiophene-2,6-diyl-alt-4-substituted-thieno[3, 4-b]thiophene-2,6-diyl] (PBDTTT). PBDTTT-based BHJ devices currently exhibit PCEs $> 7\%$ due to the exceptional tunability of the highest occupied molecular orbital (HOMO) level when electron-withdrawing functional groups are added to the polymer.[6,18] Other low bandgap polymers which show promise for use in high PCE BHJ devices include PCPDTBT, PTB, PTPTB, PEOPT, and PFDTBT.[10,19]

While many current research efforts are focused on exploiting the chemical tunability of low bandgap polymers for achieving high PCE devices,[6] even significant improvements in PCE will not enable widespread

OPV commercialization if device stabilities remain low. A variety of degradation mechanisms have been identified in traditional BHJ devices such as those based on PPV and P3HT, but the stability of devices composed of low bandgap materials remains poorly understood. Characterization of specific degradation processes in BHJ devices is difficult because of the number of different materials involved and the diverse range of optical, thermal, electronic, and chemical processes that take place inside each device layer. Phenomena commonly associated with BHJ degradation include diffusion of molecular oxygen and water into the photoactive layer, photo-induced chemical reactions in the active layer, diffusion of buffer layer and electrode materials into the active layer, morphological changes in the active layer, oxidation of electrodes, and macroscopic encapsulation changes such as delamination.[10] Each of these degradation mechanisms is catalyzed by exposure to elevated temperatures and incident light, which are ubiquitous conditions during photovoltaic device operation. The wide range in time scales at which these degradation processes occur (minutes to years), coupled with the interrelatedness between them generally makes it difficult to achieve a quantitative analysis of the effect of specific degradation mechanisms on overall device performance.[20] Understanding the source of degradation processes, which device components they affect, and the measures that can be taken to mitigate them is critical for moving low bandgap OPVs toward commercialization.

Device lifetimes are often characterized by the amount of time that passes before the device performance drops below a specified fraction of its original value. Lifetimes can be quantified by T80 or T50 values, which correspond to the times required for devices to degrade to 80% or 50%, respectively, of their initial performances. Advanced encapsulation techniques have allowed for P3HT:fullerene lifetimes to exceed 5000 hours (roughly 3 years in realistic outdoor conditions)[21] and the recent milestone of the 100,000 hour operational lifetime of an organic light-emitting diode (OLED) suggests that 5 year outdoor lifetimes for OPVs are within reach.[22]

2 Review of Common Degradation Processes and Characterization Methods

This section outlines current device degradation models and the most commonly used experimental techniques for investigating device stability. Methods for assessing the electronic, chemical, morphological, and structural stability of BHJ devices are described. Using a variety of techniques to achieve full structural-functional characterization of device materials provides insight into both extrinsic (i.e. elevated temperature, UV illumination, high humidity) and intrinsic (interactions between different device materials) sources of device degradation. The most commonly-studied environmental stress conditions and their effects on device performance are summarized in Table 1 and are further described in the following sections. Finally, an experimental proposal is outlined for identifying mechanisms of degradation and characterizing their contribution to overall device performance.

It should be noted that while the primary purpose of this study is to provide an experimental proposal for the characterization of degradation mechanisms in BHJ devices composed specifically of low bandgap semiconductors, the experimental techniques and degradation mechanisms described here are generally applicable to a wide range of organic thin film (OTF) optoelectronic devices. The current study therefore provides a flexible framework with which to study the structural-functional evolution of materials in a variety of devices, including other types of OPVs, OLEDs, and OTF transistors.

Table 1: Stress conditions and their effects on BHJ OPV device materials

Stress condition	Effect on device
Elevated temperatures/ thermal cycling	material diffusion between layers, thermally-induced chemical reactions, phase transitions and crystallization in photoactive materials
Oxygen exposure	oxidation of electrodes, oxidation reactions in active layer materials, scission of polymer chains, unintentional active material crosslinking, polymer side chain cleavage
Water/humidity exposure	water diffusion into active layer, incorporation of OH groups in active layer structures, polymer swelling and displacement
UV exposure	exciton quenching, photochemical oxidation, photoinduced charge transfer complex formation
Mechanical stress	morphological changes, delamination, crack formation in electrodes

The most commonly used experimental techniques for studying degradation mechanisms in BHJ devices are summarized in Table 2, as adapted from Grossiord et al.[23] Each technique is characterized as a method for measuring electrical/chemical degradation, morphological degradation, or both. Included with the commonly used techniques are others which show promise for BHJ degradation investigations, including the quartz crystal microbalance (QCM) and neutron reflectivity (NR). The use of these techniques will be described further in the following sections.

2.1 Current-Voltage Characteristics

The most fundamental measure of photovoltaic device performance is the current-voltage (J-V) characteristic. The values of multiple device parameters, including PCE, open-circuit voltage (V_{oc}), short circuit current density (J_{sc}), maximum power output (P_{max}), and fill factor (FF) can be extracted from each J-V curve. The evolution of these parameters in response to changing environmental conditions and device age can yield important information about the source and severity of different degradation mechanisms occurring inside the device.

Studying environmentally-induced device degradation requires that measurements be carried out in controlled environments in which gas concentration, humidity, device temperature, and light intensity are varied. Environmental control allows for accelerated lifetime testing (ALT), a valuable tool for characterization of device stability. In typical ALT experiments, overexposure to severe environmental conditions drives devices to early failure. This allows for predictions of average device lifetime under standard operating conditions even if the lifetime is on the order of years. ALT often includes the use of 85-85 conditions in which the device under test (DUT) is held at 85°C and 85% relative humidity (RH) under unfiltered UV light while device operating parameters extracted from the J-V characteristics are monitored as a function of time.[11,24]

When device degradation is primarily the result of a first order kinetics reaction, the value $P(t)$ of a

Table 2: Common methods for characterizing degradation mechanisms. Characterization is designated as **EC** (electrical-chemical), **M** (morphological), or **Both**.

Experimental technique	Device characterization
Current-voltage (J-V) characteristics	**EC**: comprehensive device performance, electrical properties
Photoluminescence (PL)	**EC**: formation of charge transfer states, surface chemical states
X-ray photoelectron spectroscopy (XPS)	**EC**: quantitative analysis of surface chemical states, sorption processes
Time of flight secondary ion mass spectroscopy (TOF-SIMS)	**EC**: sensitive, qualitative analysis of surface chemical states, sorption
Quartz crystal microbalance (QCM)	**Both**: sorption kinetics, reversibility
Size exclusion chromatography (SEC)	**Both**: polymer chain scission, photo-induced material crosslinking
Conductive atomic force microscopy (C-AFM)	**Both**: phase separation and trap state formation in active layer
Kelvin probe force microscopy (KPFM)	**Both**: work function and phase separation in photoactive layer
Optical Spectroscopy	**Both**: crystallinity, polymer scission
Thermogravimetric analysis (TGA)	**Both**: sorption/desorption, active material decomposition
Accelerated lifetime testing (ALT)	**Both**: device lifetime determination, stability of active materials
Electroluminescence (EL)	**Both**: electrode oxidation, trap states, spatially-resolved delamination
Thermography	**Both**: trap states, pinholes, spatially-resolved delamination
Impedance spectroscopy (IS)	**Both**: active layer crystallinity, trap state formation, delamination
Neutron reflectivity (NR)	**Both**: surface composition, structure, sorption and diffusion kinetics
Atomic force microscopy (AFM)	**M**: surface morphology, electrode pinholes and cracks
Transmission electron microscopy (TEM)/ Scanning electron microscopy (SEM)	**M**: phase separation and crystallinity in cross-section of active layer
Differential scanning calorimetry (DSC)	**M**: identification of polymer/ fullerene phase transitions
X-ray diffraction (XRD)	**M**: phase transitions, crystallinity, surface composition of active layer
Neutron diffraction	**M**: phase transitions, crystallinity, surface composition of active layer

performance measure such as PCE or FF can often be related to the initial performance P_0 by $P(t) = P_0 e^{-t/\tau}$. Determining the time constant τ for each operating parameter as a function of exposure time to an environmental stress (i.e. elevated temperature, high humidity, UV illumination) can provide a quantitative measure of both the severity of the external stress on device performance and the relative time scale at which the stress induces device performance loss. Comparing τ values between different devices also makes it possible to quantify the effects of using encapsulation, buffer layers, or different polymer-fullerene species on lifetime.

One result of device degradation that is often observed in J-V characteristics is the appearance of an S-shaped feature which contains an inflection point in the forward bias quadrant of the J-V curve. The source of this degradation mechanism remains poorly understood. Some S-shape features which decrease device PCE by 20% have been observed by Mateker et al. in dark inert conditions only 7 days after device fabrication, suggesting that they arise from surface dipole formation, energy barriers, or charge accumulation at active layer-electrode interfaces.[25] However, Guerrero et al. report that S-shaped features are absent in devices left in the dark, which indicates that degradation of metal contacts are not responsible for S-shapes, but rather photo-induced chemical and morphological changes in the active layer.[26] Improving polymer purification before device fabrication has been shown to increase device lifetime and reduce the severity of S-shape formation, which suggests that low weight organic impurities like small molecule polymer byproducts, oligomers, and monomers are responsible for the rapid development of S-shaped features in J-V measurements. A detailed study of the evolution of electrical characteristics in controlled environments must be undertaken before the sources and kinetics of S-shape formation are properly understood.

2.2 Chemical Stability of the Active Layer

Perhaps the most important factor for device lifetime is chemical stability of the active layer materials.[27] Chemical processes which occur in the active layer include photo-induced and thermally-induced reactions between photoactive materials, reactions between active materials and atmospheric oxygen and water, and reactions between active materials and electrode and buffer layer materials.

It is widely recognized that chemical degradation in the active layer results primarily from interactions between active materials and molecular oxygen. Interactions with oxygen cause band structure modifications in the organic materials resulting in altered charge carrier mobilities, trap states, and exciton dissociation rates.[10] Perhaps even more significant, oxidation reactions can induce polymer rearrangement, scission, side chain cleavage, or undesirable crosslinking. Many of these processes can result in the loss of polymer π conjugation, which represents the primary source of exciton quenching (photobleaching) in the active layer.[28] Photodegradation of conjugated polymers occurs primarily through interactions with singlet oxygen ($^1O_2$) and superoxide (O_2^-). UV light-induced electron transfer from polymer triplet excited states to triplet O_2 can result in the formation of $^1O_2$, which upon reaction with active layer materials often results in destruction of polymer π-conjugation.[29] This process ruptures polymer backbones but may leave side chains relatively intact, resulting in the formation of a variety of oxidized polymer systems.[30] Photo-induced electron transfer to O_2 can lead to the creation of O_2^-, which has the ability to initiate a radical chain reaction in active polymers. This leads to irreversible reductions in both charge carrier mobility and light absorption by the photoactive blend.[8]

Because of their widespread use in traditional BHJ devices, degradation of polythiophenes has been

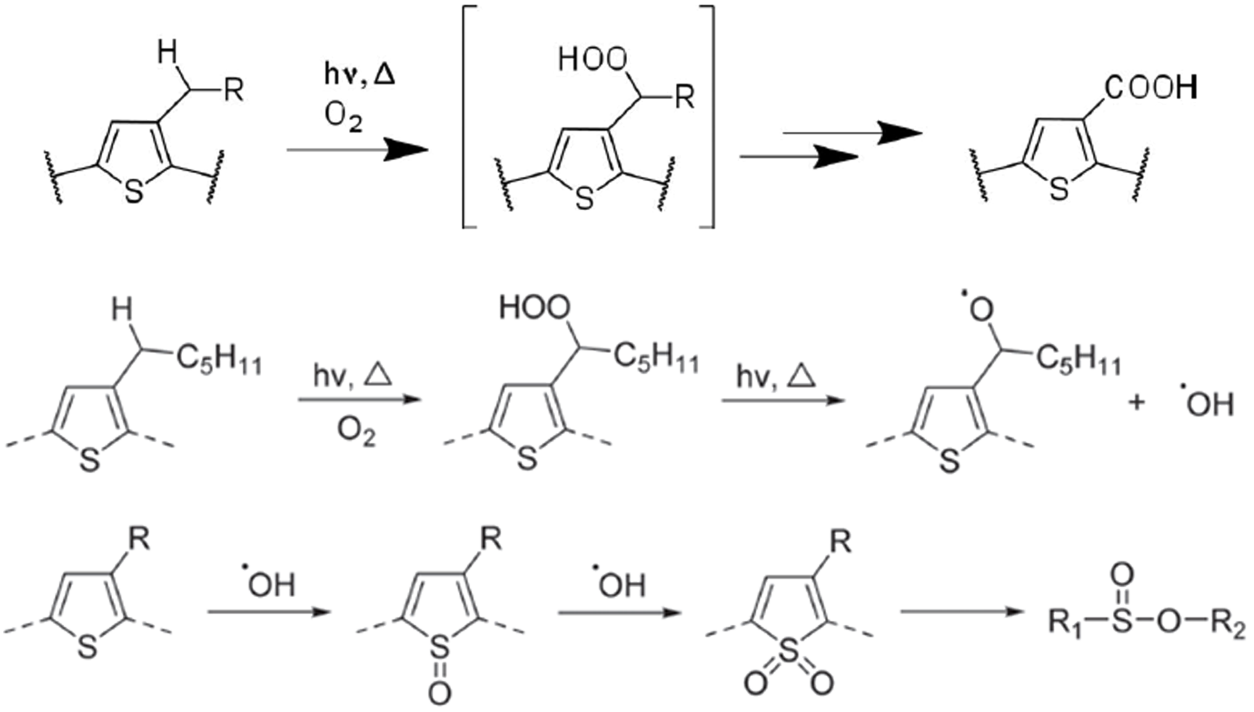

Figure 1: Common oxidation reactions in polythiophenes. Figure adapted from Bundgaard et al. and Jorgensen et al.[27,31]

studied extensively. Some of the most commonly observed oxygen-induced polythiophene reactions are shown in Figure 1. These reactions can result in side chain cleavage (top), production of free radicals (middle), and scission of aromatic rings (bottom), all of which strongly inhibit charge carrier mobility. It is believed that these reactions are common among nearly all conjugated polymers,[27] but that low bandgap materials may be especially prone to oxidation because of their particular susceptibility to photoexcitation.

One of the most frequently observed active layer degradation processes results from the interaction between oxygen and alkyl side chains.[27] This reaction is prevalent in traditional conjugated polymers like PPVs and polythiophenes as well as low bandgap materials like polyfluorenes. Side chain reactions often begin when UV illumination initiates a radical reaction at the α carbon of the alkyl side chain,[30] as depicted in Figure 2 for a low bandgap polyfluorene. This process can lead to side chain cleavage and even result in loss of π-conjugation. Cleaved side chain materials dispersed throughout the active layer act as impurities which impede charge carrier migration and reduce the D-A interfacial area, resulting in lower exciton dissociation efficiency. It has been demonstrated that impurities introduced into the active layer act as significant impediments for maintaining device stability. The exclusion of organic small molecules from the active layer during film fabrication has been shown to dramatically improve device lifetimes, which suggests that interactions between cleaved side chain impurities and active materials can strongly contribute to device degradation.[25]

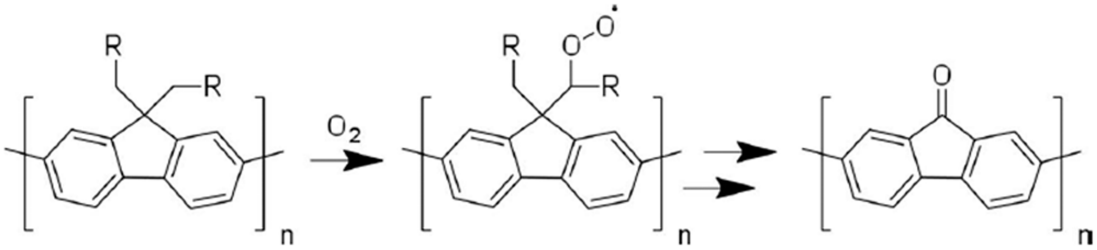

Figure 2: Oxidation-induced side chain cleavage in low bandgap polyfluorene derivatives. Figure adapted from Bundgaard et al. and Jorgensen et al.[27,31]

The degradation of conjugated polymers under solar illumination in the presence of O_2 and H_2O is often studied by UV-vis and IR spectroscopies. By calculating the number of photons absorbed by different polymers over time, Manceau et al. established the relative rate of photodegradation for multiple polymers.[33] This information was used to create a ranking of polymer stabilities, which confirmed that polymer side chains are responsible for a significant majority of photochemical degradation in polymer films.[31] The superior stability of polymers with thiophene moities, rather than carbazole or dialkoxybenzene groups, indicates that stability is greatly improved in active later materials that are not composed of easily cleavable bonds. This result suggests that chemical-structural features, such as polymer crystallinity and side chain geometry have a stronger effect on device stability than purely electronic features such as HOMO level or bandgap.[30]

Many experimental techniques have been used to characterize the effects of interactions between active layer materials and oxygen. Transient adsorption spectroscopy is useful for observing the presence of short-lived deep trap states such as those formed by photo-oxidation of conjugated polymers.[10] For investigating oxygen sorption on active later materials, X-ray photoelectron spectrometry (XPS) is often used to compliment time-of-flight secondary ion mass spectrometry (TOF-SIMS) measurements.[30] XPS provides chemical state information about the elemental compositions of the outer 5-10 nm of device surfaces. While XPS is quantitative in nature but not highly sensitive, TOF-SIMS is not quantitative but extremely sensitive.[20] These techniques are especially powerful when used in conjunction with isotope labeling of $^{18}O_2$ or $H_2^{18}O$, which reveals the extent of oxygen and water sorption that occurs during a specific experiment.

An initial efficiency loss (25% after ∼100 hours) observed in many BHJ devices, primarily the result of decreases in FF and V_{oc}, is generally termed the "burn-in" loss. Grazing incidence X-ray scattering (GIXS) studies have shown that the burn-in loss is not morphological in nature, and that X-ray coherence in the $\pi - \pi$ stacking direction in the photoactive layer decreases when films are heated above the glass transition temperature (T_g). It is suspected that the burn-in loss is a result of photochemically-induced enhancement of hole traps by the formation of sub-bandgap states. This process is likely related to photo-oxidation of polymer side chains, chain ends, or impurities.[36]

Photoexcitation of active layer materials can cause irreversible degradation even in the absence of oxygen. An example of this process is shown in the bottom of Figure 3, where photolysis leads to cage reactions in MDMO-PPV. UV illumination in anaerobic environments can also induce oligomerization of the fullerene $PC_{60}BM$, which helps to prevent oxygen diffusion but also leads to decreases in the D-A interfacial area.[30,32]

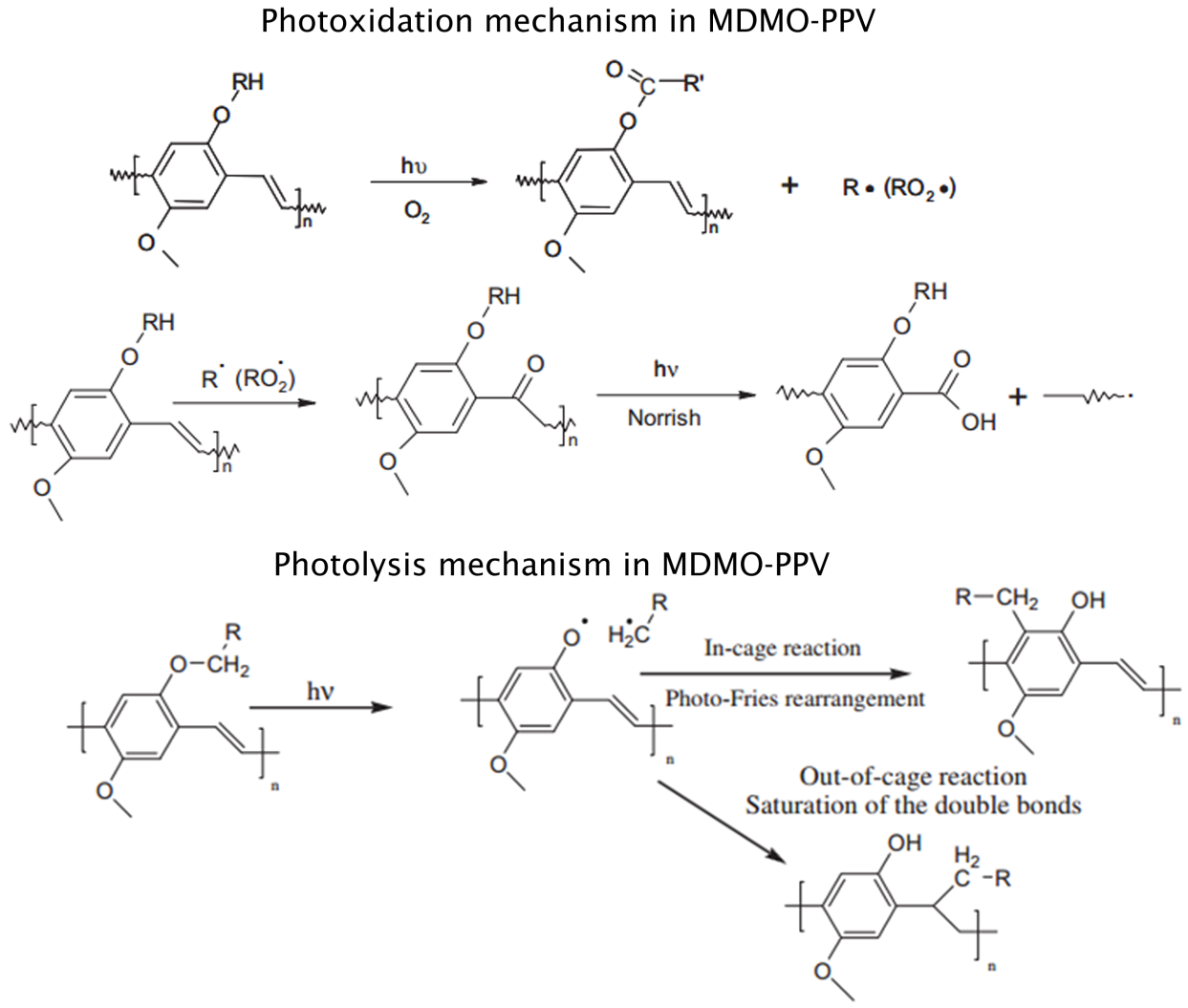

Figure 3: Photooxidation and photolysis reactions in polymer MDMO-PPV. It is likely that other lowband gap PPV derivatives undergo similar reactions. Figure adapted from Rivaton et al.[34]

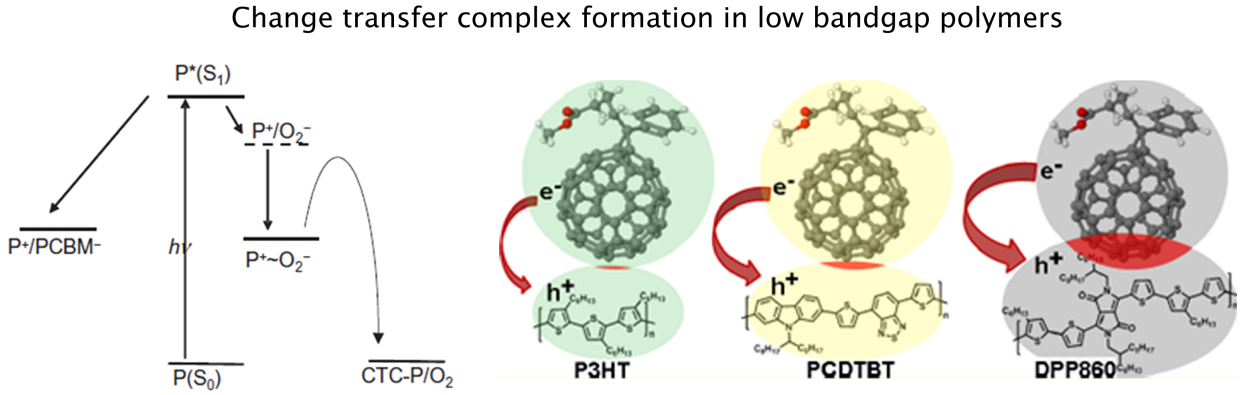

Figure 4: Left: photoexcitation of a polymer (P) and subsequent transfer of electron to PCBM or O_2. Right: a fraction of electron charge is transfered from the polymer donor to the fullerene acceptor. The charge transfer complex is particularly prevalent in low bandgap polymers, especially in the presence of O_2. Figure adapted from Aguirre et al. and Ripolles-Sanchis et al.[29,35]

One of the primary mechanisms of chemical degradation in the active layer is related to the formation of a polymer-fullerene charge transfer complex (CTC), in which a fraction of electron charge in the polymer donor is transfered to the fullerene acceptor in the electronic ground state. This phenomenon results in both exciton quenching by CTC-induced electronic defect states and decreases in visible light absorption. CTC formation is depicted in Figure 4. On the left, photoexitation of a polymer (P) results in electron transfer to PCBM or an O_2 molecule. On the right, electron charge is transferred from a polymer to fullerene. Since photoexcitation of low bandgap polymer donors occurs at low energies (< 2 eV), low bandgap PCDTBT (carbazole-based) and DPP860 (diketopyrrolopyrrole-based) polymers are more susceptible to CTC formation than traditionally-used BHJ polymers like P3HT.[29,35]

CTCs in BHJ devices are characterized using a variety of techniques. X-ray diffraction (XRD) and absorption measurements are used to correlate CTC formation with active layer crystallinity. Electrochemical cyclic voltammetry (C-V) profiling enables identification of electrically active defect sites which have formed as a result of CTC complex formation.[26] Films can be treated with thermal annealing in inert atmospheres to allow for distinction between the occurrence of irreversible chemical changes and reversible processes. Reversible performance changes are generally a result of CTC formation, not covalent bonding between the polymer and oxygen.[30] The reversibility of O_2 and H_2O doping and the role gas sorption plays in CTC formation is often studied using C-V techniques.[16]

Photochemical degradation of organic materials is investigated using a wide variety of complementary techniques including those previously mentioned. Electron spin resonance (ESR) and light-induced ESR (LESR) provide information about the rates of trap accumulation in photoactive layer materials.[37] ESR has revealed the formation of weak (reversible in vacuum or by thermal annealing) polymer-O_2^- complexes when devices are illuminated and exposed to oxygen. It is believed that UV-initiated ozone generation is responsible for this formation.[31] Laser beam induced current (LBIC) maps can be used to probe the spatial distribution of J_{sc} and charge carrier diffusion as a function of device operating time. This method can be especially useful for measuring whether photo-induced carrier mobility loss primarily occurs near pinholes or film

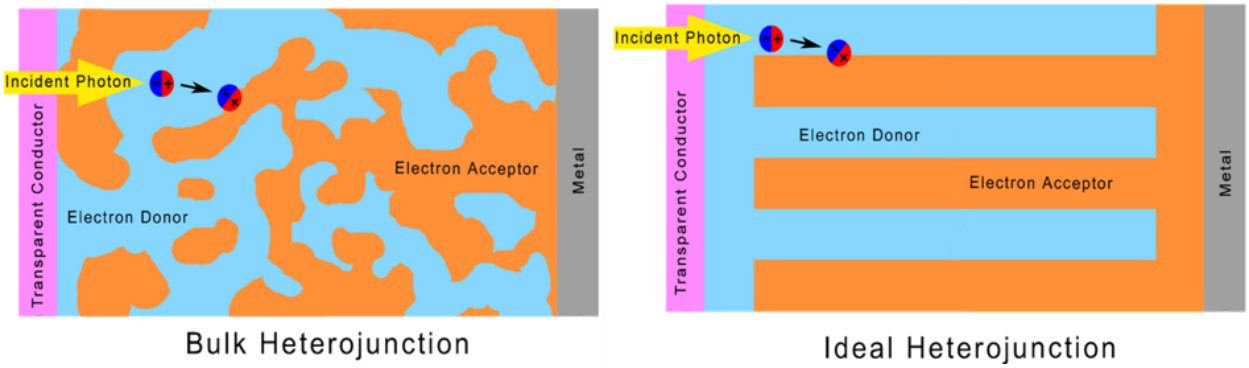

Figure 5: Left: a typical BHJ device contains a blend of donor and acceptor materials which undergo spontaneous phase separation. Right: An ideal heterojunction maximizes interfacial area while providing uninhibited conductive pathways to respective electrodes. Changes in active layer morphology can result in drastic reductions in exciton dissociation and charge carrier migration.

edges.[21] Attenuated total reflectance Fourier transform infrared spectroscopy (ATR-FTIR) has been used to quantify the degradation rates of different materials inside a single device under variable atmospheres,[10] while thermogravimetric analysis (TGA) is used for confirmation of the stability of low bandgap polymers in ambient atmospheric conditions.[16] TGA is especially useful for determining the temperature at which alkyl side groups are thermally cleaved from polymers. Variable-angle spectroscopic ellipsometry (VASE) provides information about doping concentrations and electrical conductivity, both of which change as a result chemical degradation processes in the active layer.[26] Finally, impedance spectroscopy (IS) can provide information about the recombination kinetics and transport properties of charge carriers. IS allows for investigation of electrical processes which take place at different time scales, such as carrier recombination and contact resistances (measured at low frequencies), and carrier transport (measured at high frequencies).[26]

2.3 Morphological Stability of the Active Layer

The high exciton binding energies (up to 1 eV) in organic semiconductors require that exciton dissociation occurs at the D-A interface in the photoactive device layer. This makes interfacial geometry critical for device efficiency, since exciton creation must occur within one exciton diffusion length (∼10 nm) of the D-A interface for charge extraction to occur.[6] For this reason, optimal BHJ morphology requires that every point inside the active layer lies within the exciton diffusion length from the D-A interface, and that each photoactive material is connected to its respective charge-extracting electrode by a conductive network of the same material.[8] Typical BHJ morphology and optimal device morphology are compared in Figure 5.

To optimize interfacial geometry during device fabrication, the active layer morphology is often tuned by introduction of solvent mixtures and additives or by post-deposition methods such as thermal annealing. After the desired morphology has been obtained, locking it in place is challenging because of external thermal and mechanical stresses, especially in flexible devices. This is partly due to the high mobility of fullerenes in the polymer matrix, which can conglomerate into μm-sized crystallites after short time scales (on the order of hours), leading to reductions in interfacial area and charge extraction rates.[38] Thermally-induced Ostwald ripening and polymer crystallization lead to significant polymer-fullerene phase separation, which

has been specifically identified as a primary source of J_{sc} decay in BHJ devices.[28,39]

A number of techniques have been used to characterize and monitor stress-induced changes in device morphology. Surface characterization is usually performed using atomic force microscopy (AFM), scanning transmission electron microscopy (STEM), and grazing incidence X-ray diffraction (GIXD) or grazing incidence neutron diffraction (GIND).[26] Optical microscopy methods are used to identify the formation of large-scale phase separation and domain structures.[28] Using peak force tapping and conductive AFM (C-AFM), it is possible to distinguish between fullerene and polymer structures for investigations of phase separation on the active layer surface. Although these techniques are largely limited to surface features, electron tomography, along with cross-sectional SEM or TEM images, can reveal the vertical configuration of polymer and fullerene domains throughout the entire active layer.[8] TEM, especially in bright field mode, has been used extensively to investigate the degree of phase separation in the active layer blend.[39] The combination of C-AFM with cross-sectional TEM allows for full 3-dimensional characterization of phase separation in the active layer. Utilizing these tools for morphological studies in which different films are exposed to controlled thermal and mechanical stresses can enable direct observation of the effects of each stress on morphological stability. The monitoring of phase separation by microscopy techniques also enables spatial resolution of crystal nucleation sites.

X-ray and neutron techniques allow for measurements of the crystal structure in active layer materials and active layer-electrode interfaces. Energy dispersive X-ray reflectivity (EDXR) is a nondestructive optical measurement used in conjunction with XRD and AFM analysis by Paci et al. to investigate meso-scale modifications of the surface, bulk, and metal interface of the organic layer.[40] This allows in situ imaging of complete devices during photodegradation processes to probe whether performance degradation is a direct result of photo-induced structural modification or thermal stress.[31] XRD is a standard technique for investigating the presence of different crystal phases and glass transitions, and grazing incidence wide-angle X-ray scattering (GIWAXS) has been used to identify weak ordering of PCBM.[38] For increased spatial resolution, micro-focused grazing incidence small-angle X-ray scattering (μGISAXS) is used to investigate fullerene domain size and density and its effect on J_{sc}.[41] Similarly, neutron reflectivity (NR) is useful for investigating the spatial distribution of species in the active layer, photoactive material reaction kinetics, and sorption of gases containing light elements.[32]

A variety of optical spectroscopy techniques have also been used to complement morphological investigations. UV-vis spectroscopy was used by Ning et al. to measure the change in absorption spectra after thermally-induced morphological degradation. The absorption spectra maximum increases in intensity and exhibits a redshift as a function of heating time, which indicates an increase in domain size and crystalline order.[39] Cardinaletti et al. used Raman spectroscopy to characterize the BHJ morphology changes during ALT.[8] Calorimetric techniques like rapid heat-cool calorimetry, differential scanning calorimetry (DSC), and modulated DSC provide valuable information about both ordered and disordered material phases and phase and state diagrams. DSC is often used to determine the temperature of phase transitions which occur in the active layer materials.[39] The state diagram is vital for understanding the phase separation properties of the polymer/fullerene blend, including crystallization kinetics as a function of temperature, and the T_g of each material.[8] Complementing phase transition temperature information with microscopy images and in situ X-ray or neutron measurements enables a comprehensive understanding of glass transition kinetics, phase separation, and crystallization of active layer materials.

Other methods for investigating BHJ morphology include transient photoconductivity, which is used to investigate changes in the charge transport kinetics as a result of thermal stress,[39] and laser scanning confocal fluorescence microscopy, which is often used for measurement of thermally-induced morphology changes.[42] Measuring the dielectric capacitance of active layer films using impedance spectroscopy also provides information about the degree of film crystallinity. Measured in conjunction with controlled thermal annealing, capacitance measurements can enable a quantitative relationship between the electronic properties and degree of crystallization.[42]

Several methods have shown promise for improving morphological stability of the active layer, including crosslinking and side chain functionalization of the organic materials. Under certain circumstances, these processes can increase T_g of the active layer blend to a level significantly higher than the normal operating device temperature, which results in improved morphological stability.[8,25] Crosslinking, the most common technique for stabilizing active layer morphology, is achieved by covalent bonding of two or more molecules using specific chemical species as branches. Bonding is usually induced by thermal annealing, photoinitiation, or UV curing after cross-linkable groups are introduced to the active layer materials.[28] Crosslinking can be accomplished between polymer-polymer, fullerene-fullerene, or polymer-fullerene pairs.[8] While devices employing crosslinked active materials often exhibit lower initial PECs,[38] crosslinking generally preserves the chemical stability of polymers and significantly improves morphological stability.[27] Recent efforts to increase active later stability have favored tuning fullerene crystallization affinities by modification of side chains rather than by employing crosslinked materials.[8] Side chain addition increases the fullerere T_g, which is important for the prevention of Ostwald ripening and general polymer/fullerene phase separation.[8]

Improvements in morphological stability have also been achieved through the use of active layer materials which form block copolymers.[27] Block copolymers can be synthesized by direct covalent bonding between polymers and fullerenes, which prevents thermally-induced phase separation. Schroeder et al. show that photo-induced covalent bonding between fullerene groups results in higher morphological stability in a variety of different polymer/fullerene systems[38] and Cardinaletti et al. show that light-induced fullerene dimerization can improve fullerene morphological stability.[8]

2.4 Stability of Electrodes and Buffer Layers

Degradation processes in electrodes and interfacial buffer layers can strongly affect BHJ device performance. While the purpose of electrodes is to provide ohmic electrical contacts, top electrodes also serve as important encapsulation structures for the protection of active layer materials against oxygen and water.[6,43] In this section, focus is placed on degradation mechanisms in devices which employ aluminum as a top electrode and indium tin oxide (ITO) as a bottom transparent electrode, since these materials are commonly used in a diverse range of polymer-fullerene BHJ devices.

Aluminum is attractive for use as a top electrode because of its low work function and excellent barrier properties against water diffusion. However, mechanical and thermal stresses can cause micron-sized cracks in top Al electrodes. This enables the formation of oxygen and water transport pathways from the ambient atmosphere to the photoactive layer materials.[44] Normann et al. and others show that oxygen diffusion occurs mainly through microscopic pinholes in Al while H_2O molecules favor migration between Al grains.[10] Even devices encapsulated with UV epoxy have exhibited 3% decreases in PCE while stored in nitrogen-filled gloveboxes over a 10 day period. Oxidation of the aluminum electrodes upon exposure to air is suspected

to play a role in this degradation process.[18] Water and oxygen which penetrate through the Al electrode can diffuse all the way though the active layer to reach the indium tin oxide (ITO) transparent electrode, which allows for oxidation processes to occur in every single layer of the device.[20] Degradation of the ITO layer can promote indium diffusion into the polymer/fullerene matrix, which results in electron transfer from polymer donors to indium atoms. This process decreases the difference in work function between ITO and Al, diminishes the strength of the built-in electric field at the interface between ITO and Al, and leads to loses in J_{sc} and overall device PCE.[45] Substantial changes to the work function of the ITO surface ($\sim$1 eV) can occur upon sorption of less than a monolayer of contaminant species, which often leads to the creation of electric dipoles at the interface between ITO and the photoactive materials.[45] In structures employing the fullerene PCBM as an electron acceptor, aging causes decreases in V_{oc} much more rapidly when ITO is present than when other transparent conductors are used. This has been explained by the high work function in ITO compared to that of similar transparent conductors such as the polymer blend poly(3,4-ethylenedioxythiophene):polystyrene sulfonate (PEDOT:PSS).[45]

The effects of electrode degradation are often studied by electroluminescence (EL) imaging. During EL measurements, an applied current injects charge carriers into the BHJ device, resulting in radiative recombination which is recorded by a camera. Dark regions in the EL images indicate delamination of aluminum or ITO electrodes from the active layer, or the formation of charge carrier barriers due to the oxidation of electrode materials. EL techniques allow for spatially resolved degradation imaging at the electrode-active layer interface, which enables confirmation of whether degradation occurs most often near pinholes or cracks in the electrodes. As a complementary technique, photoluminescence (PL) is used to probe changes in the quality of the active layer as a function of device lifetime. When used in conjunction, EL and PL can effectively distinguish between degradation which occurs in the bulk active layer and that which occurs at an active layer-electrode interface.[46]

The stability of interfacial buffer layer materials also plays a key role in device lifetime. Buffer layers are often deposited between electrodes and active layer materials to serve multiple functions, including formation of ohmic contacts, confinement of excitons to the active layer, and adhesion of active layers to electrodes. In flexible devices, adhesive buffer materials are often required for the prevention of dewetting and delamination since these processes cause significant performance losses when devices are subjected to mechanical stress or deformation cycling.[47] Other important functions served by buffer layers include adjustment of the work function of the electrodes, offset of the vacuum level between active layer materials and electrodes, protection of the active layer during annealing, and increasing the built-in electric field strength at device layer junctions.[48]

PEDOT:PSS is commonly used as an interfacial buffer layer material because of its desirable hole transport properties. However, its acidity and strong hygroscopic characteristics induce reactions with adjacent layers and atmospheric H_2O.[48] The high acidity (pH$\approx$1.2-2.2) of PEDOT:PSS is suspected to enhance indium diffusion into active layer materials, and the hydrophilicity of PEDOT:PSS allows for efficient transport of water from electrode surfaces through buffer layers and into active materials.[47] These processes enable rapid chemical changes in the active layer if pinholes or cracks in the electrodes are present. In high humidity environments, water sorption on PEDOT:PSS causes swelling which results in displacement of PEDOT oligmers away from PSS backbones. This results in a decrease in J_{sc} and and device PCE.[49] Interactions between PEDOT:PSS and the electrode materials can also decrease device PCEs. PEDOT:PSS-assisted transport of

water toward electrode surfaces enhances oxidation and pinhole growth in Al.[30] In a P3HT/PCBM device, it was found that the primary degradation processes which led to device failure occurred at the interface between the PEDOT:PSS electrode and the active layer. Time-of-flight secondary ion mass spectrometry (TOF-SIMS) measurements used in conjunction with isotope labeling have revealed that PEDOT:PSS blends can undergo significant phase separation, after which the PEDOT-rich phase interacts strongly with O_2.[20]

AFM is often used to characterize surface features of PEDOT:PSS and other buffer layer materials as a function of device operating time.[44] C-AFM techniques have been used to monitor changes in the surface conductivity of PEDOT:PSS films at different stages of processing/annealing to determine how the spatial distribution and quantity of conductive PEDOT domains evolves over time.[50] Utilizing this technique for degradation studies allows for a precise description of phase separation and morphological evolution of PEDOT:PSS films in response to controlled environmental stimuli such as high temperature, humidity, and mechanical bending. Deposition of PEDOT:PSS films on different device structures, including those terminated with ITO, Al electrodes, and organic active layer blends allows for a comparison between pure PEDOT:PSS behavior and behavior which arises due to PEDOT:PSS interactions with other device materials.

It is important to explore buffer layer material alternatives to PEDOT:PSS, such as polymers synthesized with the inclusion of external dopants in their structures to allow for tuning of electronic properties. Recently, polyaniline (PANI) has attracted interest as a replacement for PEDOT:PSS as a buffer layer material because of its higher chemical stability.[48] PANI-based buffer layers have exhibited lower susceptibility to the formation of electrical shorts and improved oxygen barrier characteristics over PEDOT:PSS. In initial studies, OLEDs with buffer layers composed of PANI-based materials have exhibited higher efficiencies than similar devices containing PEDOT:PSS buffers.[51] One factor which currently limits the use of PANI-based materials in BHJ OPV devices is the low solubility of PANI in common organic solvents. However, the formation of covalent bonds between PANI structures and -SOH_3 groups leads to sulfonated PANI (SPAN), which exhibits improved solubility over PANI. The high pH of SPAN-based buffer layers (pH$\approx$3.5-4) compared to that of PEDOT:PSS helps slow indium diffusion into the buffer layer. Devices with SPAN-based buffers doped with toluene sulfonic acid (SPAN-R[TSA^-]) exhibit significantly longer ($\sim$15-25%) device lifetimes than those with PEDOT:PSS. The improvement in lifetime can be attributed to the lower acidity of SPAN and its prevention of anion exchange with adjacent materials during polymer redox reactions.[48]

3 Experimental Proposal

In this section, a comprehensive approach to characterization of device degradation mechanisms is detailed. Since in most cases it is extremely difficult to distinguish between different sources of degradation when characterization of a complete device is carried out, experimental emphasis here is placed on a systematic characterization of individual device layers. Such a method is necessary for identifying the source of degradation effects which are only observable in a fully functional device, such as the presence of S-shaped J-V characteristics or the source of the burn-in loss. The experimental approach described here is novel because it incorporates both in situ structural and functional characterization while device materials are exposed to both individual environmental stresses and realistic outdoor 85-85 conditions. The proposal also relies on machine learning tools to enable high-level data analysis and predictions which are currently underutilized

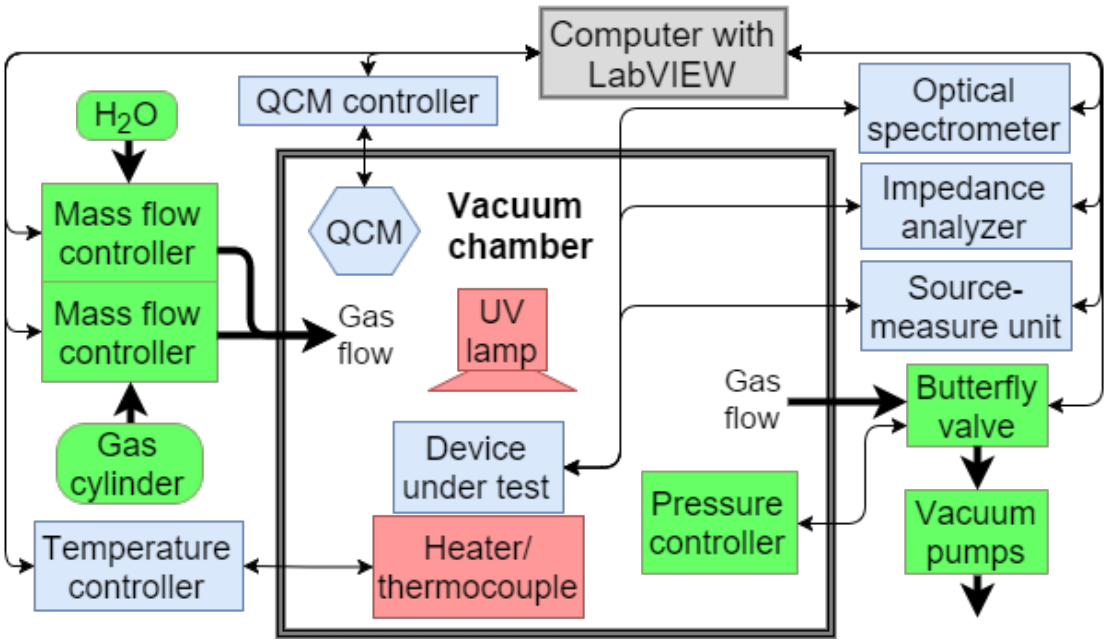

Figure 6: Environmental system used for in situ characterization of device degradation. Replication of this system at the neutron reflectivity beam line allows for full in situ diagnostics and real time monitoring of structural-functional device properties under the influence of a variety of different environmental stress conditions.

in studies on optoelectronic device degradation.

The in situ experiments described here necessitate a controlled environmental platform suitable for versatile sample testing during which a variety of external stresses can be applied. We have developed an environmental system capable of performing in situ electrical, optical, and QCM characterization under tunable simulated outdoor conditions such as elevated temperatures, UV illumination, high humidity, and oxygen rich atmospheres. The configuration of the system is shown in Figure 6. A similar system will soon be replicated for use at the SNS neutron reflectivity beam at ORNL to enable in situ structural characterization under controlled environmental conditions. For the remainder of this proposal, it is assumed that the system described in Figure 6 will contain a neutron beamline window for incident and reflected neutrons. This enables a wide suite of in situ measurements to take place inside a single chamber while a diverse configuration of environmental conditions are simulated.

Structural characterization will be accomplished using neutron reflectivity. Electrical/functional measurements will be carried out by IS using a Zahner IM6 electrochemical workstation and J-V characteristics collected by a Keithley 4200-SCS parameter analyzer. Finally, adsorption measurements will be characterized using an SRS200 QCM controller.

A general outline of the experimental proposal is depicted in Figure 7. In order to distinguish between degradation mechanisms which occur in specific device layers, three sets of samples are fabricated: active layer polymer/fullerene films, buffer layer/electrode films, and complete devices. An additional set of polymer/fullerene films are deposited on QCM crystals to allow for adsorption measurements. By measuring the characteristics of each layer individually and comparing them to the performance of complete degraded

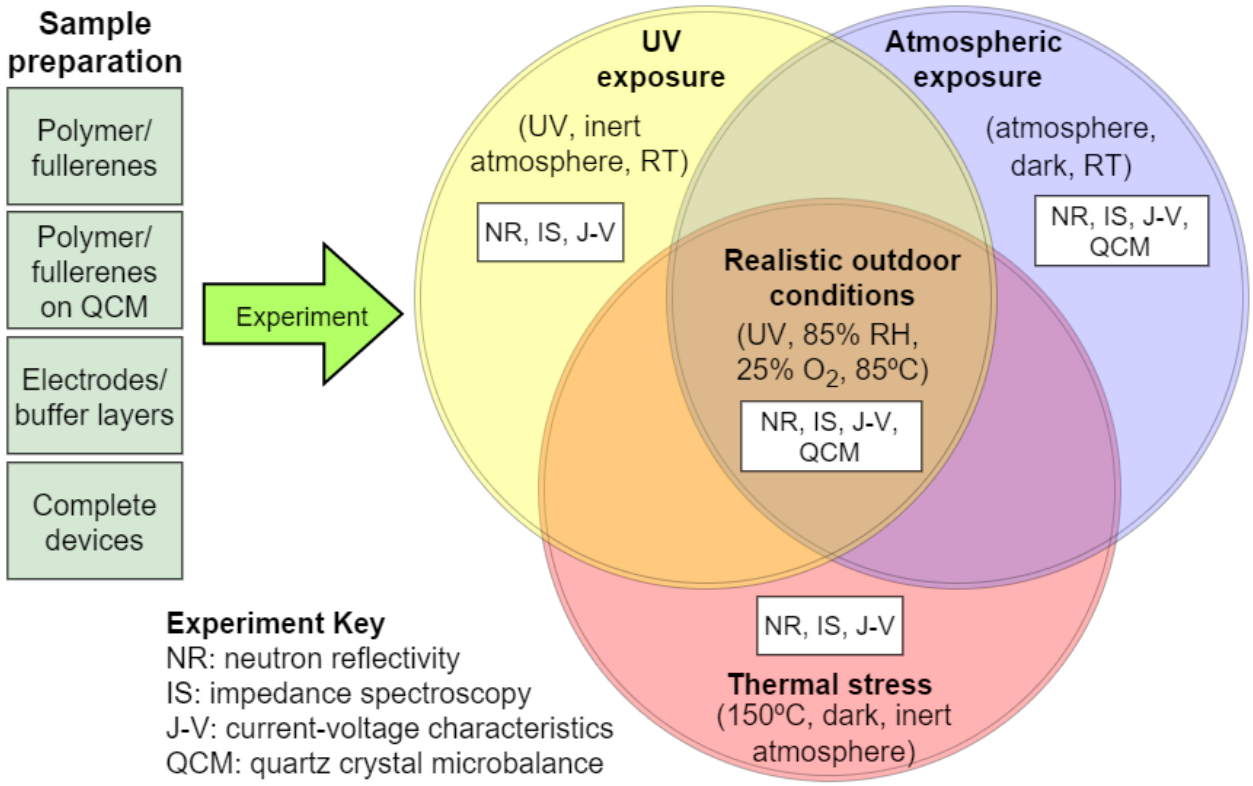

Figure 7: After samples are fabricated, they are characterized by the controlled environmental system shown in Figure 6. A series of experiments which isolate the effects of UV exposure, atmospheric exposure, and thermal stress are compared to degradation effects which are observed under realistic 85-85 conditions in which all three stresses are induced. This experimental program is carried out for individual device layers and complete devices in order to identify the specific materials in which structural-functional changes occur in response to each stress. The overall device performance degradation is then correlated with the changes that occur in each layer.

devices, it is possible to extract information about which degradation processes occur in individual materials and which processes occur as a result of interactions at device layer interfaces. For each experiment, a set of pristine samples is used to prevent convolution of degradation sources. It should be noted that not every experiment will not be performed on each sample set. For example, QCM measurements will only be performed on samples deposited on QCM crystals. All fabricated films and devices are stored under inert atmosphere in the dark at RT to minimize the degradation processes which take place before measurements are acquired.

3.1 Degradation Measurements

Before any degradation processes are intentionally initiated, it is important to acquire reference measurements with which to compare degraded films. Pristine samples placed in the environmental chamber should be fully characterized before exposed to environmental stresses. After reference characterizations of structure and electronic properties are carried out on all pristine samples, individual degradation processes are initiated. To distinguish the effects of each individual environmental stress on device performance, films and devices are exposed to a single external stress at a time. Finally, pristine samples are characterized under a combination of stresses to simulate realistic outdoor conditions. This allows for identification of nonlinear degradation effects which may not be present when stresses are applied individually but which arise only as a result of exposure to simultaneous stresses.

For thermal degradation (red circle in Figure 7), all samples are maintained in a dark inert environment and heated to 150°C, while impedance spectra, J-V characteristics, and neutron reflectivity profiles are acquired every 30 minutes or until a significant change in performance and/or structure is observed. The structural and electronic properties of each degraded sample are compared to those of pristine films. Since all thermally-induced degradation is carried out in dark inert atmospheres, any changes in structural-functional film properties can be directly correlated to thermally-induced processes.

For UV-induced degradation (yellow circle in Figure 7), samples are maintained under a calibrated UV lamp at RT in inert atmosphere. Structural characterization is carried out by NR and electrical characterization is accomplished by IS and J-V characteristics. After photo-induced degradation experiments, the structural and electronic properties of each degraded film are compared to those of pristine films. Since UV-illumination experiments are carried out in inert atmospheres at room temperature, changes in film properties that occur during this experiment can be directly attributed to photo-induced processes.

For studies of sorption-induced degradation (blue circle in Figure 7), pristine films and those deposited on QCM crystals are placed under vacuum in the dark at RT to induce gas desorption from film surfaces. The chamber is filled with O_2 (partial pressure 25%) and H_2O vapor (RH 85%) and IS, J-V, and NR measurements are acquired every 30 minutes. Neutron data is used to monitor polymer displacement as a result of sorption-induced polymer swelling, changes in crystallization, and oxygen-induced polymer scission and crosslinking between active materials. The NR results are correlated with IS data in order to quantify the effect of sorption on the electrical properties of each device component. QCM data is recorded continuously to enable a correlation between gas sorption and structural-functional changes. After all measurements are completed, the environmental chamber is placed back under vacuum and desorption of gas from each film is monitored. This provides a direct measurement of the proportion of gas which is reversibly physisorbed and that which is irreversibly chemisorbed. As a complement to traditional QCM measurements, QCM with

energy dissipation (QCM-D) can also provide valuable insight into physical and chemical changes which occur in the films. QCM-D measurements acquired during H_2O and O_2 sorption alongside the traditional QCM technique provide information about changes in the viscoelastic properties of the deposited films. Changes in viscoelasticity imply sorption-induced polymer swelling, displacement, scission, crosslinking, or the introduction of impurities as oxidation-induced side chain cleavage occurs. After sorption-induced degradation experiments, the structural and electronic properties of each degraded film are compared to those of pristine films. Since sorption experiments are carried out in dark inert atmospheres, all the changes in film properties that occur during this experiment can be directly attributed to sorption-induced degradation processes. Results from the QCM measurements are used to correlate the structural-functional changes with the amount of mass adsorbed from the atmosphere.

Although the previously described degradation experiments are designed to isolate specific effects of device stress in a systematic manner, they do not address the consequences of subjecting device materials to multiple stresses simultaneously. Realistic device degradation mechanisms are often a consequence of exposure to multiple simultaneous environmental stresses. For comparison with isolated environmental stresses, and to simulate a more realistic device environment, the effects of gas sorption are combined with UV and elevated temperature in the final experiment. This experiment simulates 85-85 conditions in which the sample is held at 85°C and 85% RH while also exposed 25% partial pressure of O_2 and UV light. Every 30 minutes, NR, IS, and J-V measurements are carried out. QCM data is acquired continuously during the duration of the experiment. After device characterization in the presence of multiple stresses is carried out, device properties are compared to those of pristine devices and those which were exposed to only one individual stress. This makes it possible to determine the specific stress that induces each degradation mechanism, and whether the individual stress itself or its combination with other stresses is the primary cause of device degradation in each layer.

For completeness, the effects of mechanical stress on device performance may also be characterized for flexible devices. All films and complete devices are fabricated on flexible substrates and maintained under inert atmospheres in the dark at room temperature. Using a servomotor to precisely control mechanical bending, devices are bent from 0° to 90° in 10° increments. At each stage during the bending process, electrical characterization using IS and J-V characteristics are carried out. At the end of the experiment, devices are returned to their original shapes and characterization is repeated. This allows for a determination of the degree to which bending induces irreversible changes in film properties.

3.2 Data Analysis

Since the experiments described here generate an enormous amount of qualitatively diverse data, it is helpful to discuss some methods of data organization and analysis. The degradation of overall device performance is primarily characterized using J-V characteristics and IS data. Parameters like V_{oc}, J_{sc}, and FF can be extracted from J-V characteristics and compared to their original values at multiple points during the degradation processes. This allows for insight into whether the most significant source of overall device degradation is induced by high temperature, UV illumination, or gas sorption, or whether these stresses have little ability influence device stability on their own and must be coupled with additional stresses to significantly impact device lifetimes.

After characterization of overall device performance has been completed, it can be correlated with struc-

tural and functional changes which are observed in each of the individual device layers. This allows for insight into which layers or layer interfaces contribute the most to overall device performance losses. With a complete understanding of the processes taking place in each layer, an entire device model can be built up from individual layers and in principle, overall performance can be predicted by changes in the properties of each of its layers. Developing a prediction of overall device performance based on the stability of each individual layer is difficult because of the large variety of processes, materials, and interactions taking place, and because an understanding of how individual components contribute to overall device performance can be extremely difficult if competing degradation mechanisms or complex nonlinear effects occur in different device layers. For this reason, it is advantageous to employ a computational analysis tool. Some tools which may be useful for application in this study are the artificial neural network (ANN) and principle component analysis (PCA).

There are a number of advantages to using ANNs for data analysis in device degradation studies. ANN predictions are based purely on empirical data (i.e. there is no need to employ a computational model), ANNs can generalize (extrapolate and interpolate) the behavior of nonlinear systems even when trends in the data are not readily apparent, and ANNs can approximate any relationship between multiple variables as long as some sort of causal relation exists, even if it cannot be readily identified.[52] There are several useful applications of ANNs which are relevant to the study of BHJ device degradation. The first is a prediction of overall device performance when performance loses in one or more device layers is identified. By training the ANN with data from a pristine device, individual pristine device layers, degraded device layers, and a degraded device, it is possible for the ANN to predict overall device performance based on the degradation conditions in an individual layer. This can be an extremely powerful diagnostic tool for investigating and predicting, for example, the effects on overall device performance of altering a single device layer.

ANNs also show value as tools for predicting device lifetimes. An ANN trained with data from pristine devices and device layers, degraded devices and device layers, and corresponding device lifetimes in the form of T80 or T50 values has the capacity to predict overall device lifetime based solely on the degree of degradation which has occurred in a single layer. This enables the possibility of rapid characterization of device lifetimes when changes in only one film, such as the photoactive layer blend, are studied. The prediction of overall device lifetime by characterization of a single layer may allow for automated ALT using a large number of films deposited on a single chip, which drastically increases the speed and lowers the cost of BHJ degradation characterization.

PCA shows promise as a tool for analysis of device degradation experiments in which multiple device materials are subjected to different combinations of environmental stresses. Although after viewing experimental data it may be obvious that functional or structural changes in device materials have occurred, the degree to which some degradation processes are either relatively insignificant or are highly correlated with other processes may not be immediately apparent. Using PCA, it is possible to reduce the number of variables in a large data set so that only the most significant variables are visible. This ensures that unnecessary focus is not placed on mechanisms which have little or no effect on overall device performance. PCA can also reveal connections between variables that are difficult to distinguished before the principal components of the data set have been identified. This allows for further insight into the performance of specific device structures as a function of individual environmental conditions such as temperature or duration of UV exposure.

4 Conclusions and Guidance for Future Directions

This study describes some of the most commonly observed degradation mechanisms in polymer-fullerene BHJ OPV devices. Using guidance from the literature, a comprehensive layer by layer strategy for monitoring in situ device degradation is developed here. Although it is well known that interactions between different device layers play a key role in device stability, little work has been done to characterize each device structure individually for the purpose of correlating overall device performance with the stability of constituent layers. The focus on in situ layer by layer structural-functional degradation characterization makes this approach far more comprehensive than the majority of other BHJ device stability studies. In addition, underutilized computational tools such as neural networks and PCA analysis are described. Combining efficient data analysis techniques with in situ structural-functional characterization provides a novel and powerful approach to identifying stability issues in OPV devices.

As the next generation of high PCE polymer-fullerene BHJ devices is designed, it is critical that researchers keep device stability in mind. The present study has illuminated some promising directions for future development and concludes by offering some final recommendations for improving the stability of the next generation of devices. Effective encapsulation techniques must be developed for preventing oxygen and water from entering photoactive layers by diffusion through outer electrodes. For the protection of active layer materials against electrodes and air, it is essential to develop interfacial layers which exhibit improved intrinsic stability over those currently used, such as PEDOT:PSS. Crosslinking, block copolymers, and light-induced oligomerization of fullerenes are techniques which should be further investigated for increasing T_g and improving active layer morphological stability. The possibility of introducing functionalized side-chains for reducing thermally-induced fullerene aggregation in the active layer should be pursued, while polymers with easily-cleavable side chains should by avoided. Polymer purification processes should be refined to allow for high purity materials which are devoid of low molecular weight species.

As PCEs in OPVs increase to levels which make BHJ devices feasible for large-scale commercialization, improving device stability becomes more urgent. The use of systematic structural-functional characterization of BHJ device materials is required for a comprehensive understanding of degradation mechanisms in these devices. Ultimately, it is expected that this will enable widespread OVP implementation for the realization of an abundant low cost renewable energy source.

References

[1] Richard M Swanson. Approaching the 29% limit efficiency of silicon solar cells. In *Photovoltaic Specialists Conference, 2005. Conference Record of the Thirty-first IEEE*, pages 889–894. IEEE, 2005.

[2] Harald Hoppe and Niyazi Serdar Sariciftci. Organic solar cells: An overview. *Journal of Materials Research*, 19(07):1924–1945, 2004.

[3] Mihaela Girtan and M Rusu. Role of ito and pedot: Pss in stability/degradation of polymer: fullerene bulk heterojunctions solar cells. *Solar Energy Materials and Solar Cells*, 94(3):446–450, 2010.

[4] Jeffery Peet, Jin Young Kim, Nelson E Coates, Wang Li Ma, Daniel Moses, Alan J Heeger, and Guillermo C Bazan. Efficiency enhancement in low-bandgap polymer solar cells by processing with alkane dithiols. *Nature materials*, 6(7):497–500, 2007.

[5] Jean Roncali. Molecular bulk heterojunctions: an emerging approach to organic solar cells. *Accounts of chemical research*, 42(11):1719–1730, 2009.

[6] Bernard Kippelen and Jean-Luc Brédas. Organic photovoltaics. *Energy & Environmental Science*, 2(3):251–261, 2009.

[7] Sung Heum Park, Anshuman Roy, Serge Beaupre, Shinuk Cho, Nelson Coates, Ji Sun Moon, Daniel Moses, Mario Leclerc, Kwanghee Lee, and Alan J Heeger. Bulk heterojunction solar cells with internal quantum efficiency approaching 100%. *Nature photonics*, 3(5):297–302, 2009.

[8] Ilaria Cardinaletti, Jurgen Kesters, Sabine Bertho, Bert Conings, Fortunato Piersimoni, Jan D'Haen, Laurence Lutsen, Milos Nesladek, Bruno Van Mele, Guy Van Assche, et al. Toward bulk heterojunction polymer solar cells with thermally stable active layer morphology. *Journal of Photonics for Energy*, 4(1):040997–040997, 2014.

[9] Jonathan D Servaites, Mark A Ratner, and Tobin J Marks. Organic solar cells: a new look at traditional models. *Energy & Environmental Science*, 4(11):4410–4422, 2011.

[10] Christoph J Brabec, Srinivas Gowrisanker, Jonathan JM Halls, Darin Laird, Shijun Jia, and Shawn P Williams. Polymer–fullerene bulk-heterojunction solar cells. *Advanced Materials*, 22(34):3839–3856, 2010.

[11] S Schuller, P Schilinsky, J Hauch, and CJ Brabec. Determination of the degradation constant of bulk heterojunction solar cells by accelerated lifetime measurements. *Applied Physics A*, 79(1):37–40, 2004.

[12] Carsten Deibel and Vladimir Dyakonov. Polymer–fullerene bulk heterojunction solar cells. *Reports on Progress in Physics*, 73(9):096401, 2010.

[13] Renee Kroon, Martijn Lenes, Jan C Hummelen, Paul WM Blom, and Bert De Boer. Small bandgap polymers for organic solar cells (polymer material development in the last 5 years). *Polymer Reviews*, 48(3):531–582, 2008.

[14] Sean E Shaheen, David S Ginley, and Ghassan E Jabbour. Organic-based photovoltaics: toward low-cost power generation. *MRS bulletin*, 30(01):10–19, 2005.

[15] Pierre-Luc T Boudreault, Ahmed Najari, and Mario Leclerc. Processable low-bandgap polymers for photovoltaic applications†. *Chemistry of Materials*, 23(3):456–469, 2010.

[16] Jianhui Hou, Hsiang-Yu Chen, Shaoqing Zhang, Gang Li, and Yang Yang. Synthesis, characterization, and photovoltaic properties of a low band gap polymer based on silole-containing polythiophenes and 2, 1, 3-benzothiadiazole. *Journal of the American Chemical Society*, 130(48):16144–16145, 2008.

[17] Dong Hwan Wang, Keum Hwan Park, Jung Hwa Seo, Jason Seifter, Ji Hye Jeon, Jung Kyu Kim, Jong Hyeok Park, O Ok Park, and Alan J Heeger. Enhanced power conversion efficiency in pcdtbt/pc70bm bulk heterojunction photovoltaic devices with embedded silver nanoparticle clusters. *Advanced Energy Materials*, 1(5):766–770, 2011.

[18] Hsiang-Yu Chen, Jianhui Hou, Shaoqing Zhang, Yongye Liang, Guanwen Yang, Yang Yang, Luping Yu, Yue Wu, and Gang Li. Polymer solar cells with enhanced open-circuit voltage and efficiency. *Nature Photonics*, 3(11):649–653, 2009.

[19] Christoph Winder and Niyazi Serdar Sariciftci. Low bandgap polymers for photon harvesting in bulk heterojunction solar cells. *Journal of Materials Chemistry*, 14(7):1077–1086, 2004.

[20] Kion Norrman, Morten V Madsen, Suren A Gevorgyan, and Frederik C Krebs. Degradation patterns in water and oxygen of an inverted polymer solar cell. *Journal of the American Chemical Society*, 132(47):16883–16892, 2010.

[21] Craig H Peters, IT Sachs-Quintana, John P Kastrop, Serge Beaupre, Mario Leclerc, and Michael D McGehee. High efficiency polymer solar cells with long operating lifetimes. *Advanced Energy Materials*, 1(4):491–494, 2011.

[22] Gufeng He, Carsten Rothe, Sven Murano, Ansgar Werner, Olaf Zeika, and Jan Birnstock. White stacked oled with 38 lm/w and 100,000-hour lifetime at 1000 cd/m2 for display and lighting applications. *Journal of the Society for Information Display*, 17(2):159–165, 2009.

[23] Nadia Grossiord, Jan M Kroon, Ronn Andriessen, and Paul WM Blom. Degradation mechanisms in organic photovoltaic devices. *Organic Electronics*, 13(3):432–456, 2012.

[24] Frederik C Krebs, Suren A Gevorgyan, Bobak Gholamkhass, Steven Holdcroft, Cody Schlenker, Mark E Thompson, Barry C Thompson, Dana Olson, David S Ginley, Sean E Shaheen, et al. A round robin study of flexible large-area roll-to-roll processed polymer solar cell modules. *Solar Energy Materials and Solar Cells*, 93(11):1968–1977, 2009.

[25] William R Mateker, Jessica D Douglas, Clément Cabanetos, IT Sachs-Quintana, Jonathan A Bartelt, Eric T Hoke, Abdulrahman El Labban, Pierre M Beaujuge, Jean MJ Fréchet, and Michael D McGehee. Improving the long-term stability of pbdttpd polymer solar cells through material purification aimed at removing organic impurities. *Energy & Environmental Science*, 6(8):2529–2537, 2013.

[26] Antonio Guerrero, Hamed Heidari, Teresa S Ripolles, Alexander Kovalenko, Martin Pfannmöller, Sara Bals, Louis-Dominique Kauffmann, Juan Bisquert, and Germà Garcia-Belmonte. Shelf life degradation of bulk heterojunction solar cells: Intrinsic evolution of charge transfer complex. *Advanced Energy Materials*, 5(7), 2015.

[27] Eva Bundgaard, Martin Helgesen, Jon E Carlé, Frederik C Krebs, and Mikkel Jørgensen. Advanced functional polymers for increasing the stability of organic photovoltaics. *Macromolecular Chemistry and Physics*, 214(14):1546–1558, 2013.

[28] Guillaume Wantz, Lionel Derue, Olivier Dautel, Agnès Rivaton, Piétrick Hudhomme, and Christine Dagron-Lartigau. Stabilizing polymer-based bulk heterojunction solar cells via crosslinking. *Polymer international*, 63(8):1346–1361, 2014.

[29] Aránzazu Aguirre, SCJ Meskers, RAJ Janssen, and H-J Egelhaaf. Formation of metastable charges as a first step in photoinduced degradation in π-conjugated polymer: fullerene blends for photovoltaic applications. *Organic Electronics*, 12(10):1657–1662, 2011.

[30] Vida Turkovic, Sebastian Engmann, Daniel AM Egbe, Marcel Himmerlich, Stefan Krischok, Gerhard Gobsch, and Harald Hoppe. Multiple stress degradation analysis of the active layer in organic photovoltaics. *Solar Energy Materials and Solar Cells*, 120:654–668, 2014.

[31] Mikkel Jørgensen, Kion Norrman, Suren A Gevorgyan, Thomas Tromholt, Birgitta Andreasen, and Frederik C Krebs. Stability of polymer solar cells. *Advanced Materials*, 24(5):580–612, 2012.

[32] Him Cheng Wong, Zhe Li, Ching Hong Tan, Hongliang Zhong, Zhenggang Huang, Hugo Bronstein, Iain McCulloch, Joao T Cabral, and James R Durrant. Morphological stability and performance of polymer–fullerene solar cells under thermal stress: The impact of photoinduced pc60bm oligomerization. *ACS nano*, 8(2):1297–1308, 2014.

[33] Matthieu Manceau, Eva Bundgaard, Jon E Carlé, Ole Hagemann, Martin Helgesen, Roar Søndergaard, Mikkel Jørgensen, and Frederik C Krebs. Photochemical stability of π-conjugated polymers for polymer solar cells: a rule of thumb. *Journal of Materials Chemistry*, 21(12):4132–4141, 2011.

[34] Agnès Rivaton, Sylvain Chambon, Matthieu Manceau, Jean-Luc Gardette, Noëlla Lemaître, and Stéphane Guillerez. Light-induced degradation of the active layer of polymer-based solar cells. *Polymer Degradation and Stability*, 95(3):278–284, 2010.

[35] Teresa Ripolles-Sanchis, Sonia R Raga, Antonio Guerrero, Matthias Welker, Mathieu Turbiez, Juan Bisquert, and Germa Garcia-Belmonte. Molecular electronic coupling controls charge recombination kinetics in organic solar cells of low bandgap diketopyrrolopyrrole, carbazole, and thiophene polymers. *The Journal of Physical Chemistry C*, 117(17):8719–8726, 2013.

[36] Craig H Peters, IT Sachs-Quintana, William R Mateker, Thomas Heumueller, Jonathan Rivnay, Rodigo Noriega, Zach M Beiley, Eric T Hoke, Alberto Salleo, and Michael D McGehee. The mechanism of burn-in loss in a high efficiency polymer solar cell. *Advanced Materials*, 24(5):663–668, 2012.

[37] Lyubov A Frolova, Natalia P Piven, Diana K Susarova, Alexander V Akkuratov, Sergey D Babenko, and Pavel A Troshin. Esr spectroscopy for monitoring the photochemical and thermal degradation of conjugated polymers used as electron donor materials in organic bulk heterojunction solar cells. *Chemical Communications*, 51(12):2242–2244, 2015.

[38] Bob C Schroeder, Zhe Li, Michael A Brady, Gregório Couto Faria, Raja Shahid Ashraf, Christopher J Takacs, John S Cowart, Duc T Duong, Kar Ho Chiu, Ching-Hong Tan, et al. Enhancing fullerene-based solar cell lifetimes by addition of a fullerene dumbbell. *Angewandte Chemie International Edition*, 53(47):12870–12875, 2014.

[39] Yu Ning, Longfeng Lv, Yunzhang Lu, Aiwei Tang, Yufeng Hu, Zhidong Lou, Feng Teng, and Yanbing Hou. Investigation on thermal degradation process of polymer solar cells based on blend of pbdttt-c and bm. *International Journal of Photoenergy*, 2014, 2014.

[40] B Paci, A Generosi, D Bailo, V Rossi Albertini, and R De Bettignies. Discriminating bulk, surface and interface aging effects in polymer-based active materials for efficient photovoltaic devices. *Chemical Physics Letters*, 494(1):69–74, 2010.

[41] Christoph J Schaffer, Claudia M Palumbiny, Martin A Niedermeier, Christian Jendrzejewski, Gonzalo Santoro, Stephan V Roth, and Peter Müller-Buschbaum. A direct evidence of morphological degradation on a nanometer scale in polymer solar cells. *Advanced Materials*, 25(46):6760–6764, 2013.

[42] Marta Tessarolo, Antonio Guerrero, Desta Gedefaw, Margherita Bolognesi, Mario Prosa, Xiaofeng Xu, Mahdi Mansour, Ergang Wang, Mirko Seri, Mats R Andersson, et al. Predicting thermal stability of organic solar cells through an easy and fast capacitance measurement. *Solar Energy Materials and Solar Cells*, 141:240–247, 2015.

[43] Serap Günes, Helmut Neugebauer, and Niyazi Serdar Sariciftci. Conjugated polymer-based organic solar cells. *Chemical reviews*, 107(4):1324–1338, 2007.

[44] Martin Kaltenbrunner, Matthew S White, Eric D Głowacki, Tsuyoshi Sekitani, Takao Someya, Niyazi Serdar Sariciftci, and Siegfried Bauer. Ultrathin and lightweight organic solar cells with high flexibility. *Nature communications*, 3:770, 2012.

[45] Mihaela Girtan and M Rusu. Role of ito and pedot: Pss in stability/degradation of polymer: fullerene bulk heterojunctions solar cells. *Solar Energy Materials and Solar Cells*, 94(3):446–450, 2010.

[46] M Seeland, R Rösch, and H Hoppe. Luminescence imaging of polymer solar cells: Visualization of progressing degradation. *Journal of Applied Physics*, 109(6):064513, 2011.

[47] Hin-Lap Yip and Alex K-Y Jen. Recent advances in solution-processed interfacial materials for efficient and stable polymer solar cells. *Energy & Environmental Science*, 5(3):5994–6011, 2012.

[48] Gopalan Sai-Anand, Anantha-Iyengar Gopalan, Kwang-Pill Lee, Swaminathan Venkatesan, Byoung-Ho Kang, Sang-Won Lee, Jae-Sung Lee, Qiquan Qiao, Dae-Hyuk Kwon, and Shin-Won Kang. A futuristic strategy to influence the solar cell performance using fixed and mobile dopants incorporated sulfonated polyaniline based buffer layer. *Solar Energy Materials and Solar Cells*, 141:275–290, 2015.

[49] Jie Liu, Mangilal Agarwal, Kody Varahramyan, Ernest S Berney, and Wayne D Hodo. Polymer-based microsensor for soil moisture measurement. *Sensors and Actuators B: Chemical*, 129(2):599–604, 2008.

[50] Liam SC Pingree, Bradley A MacLeod, and David S Ginger. The changing face of pedot: Pss films: Substrate, bias, and processing effects on vertical charge transport†. *The Journal of Physical Chemistry C*, 112(21):7922–7927, 2008.

[51] RWT Higgins, NA Zaidi, and AP Monkman. Emeraldine base polyaniline as an alternative to poly (3, 4-ethylenedioxythiophene) as a hole-transporting layer. *Advanced Functional Materials*, 11(6):407–412, 2001.

[52] Guoqiang Zhang, B Eddy Patuwo, and Michael Y Hu. Forecasting with artificial neural networks: The state of the art. *International journal of forecasting*, 14(1):35–62, 1998.